Molecules in a Bose-Einstein Condensate
Roahn Wynar, *et al.*
Science **287**, 1016 (2000);
DOI: 10.1126/science.287.5455.1016

This copy is for your personal, non-commercial use only.

If you wish to distribute this article to others, you can order high-quality copies for your colleagues, clients, or customers by clicking here.

Permission to republish or repurpose articles or portions of articles can be obtained by following the guidelines here.

The following resources related to this article are available online at www.sciencemag.org (this information is current as of October 28, 2010):

Updated information and services, including high-resolution figures, can be found in the online version of this article at:
http://www.sciencemag.org/cgi/content/full/287/5455/1016

This article **cites 2 articles**, 1 of which can be accessed for free:
http://www.sciencemag.org/cgi/content/full/287/5455/1016#otherarticles

This article has been **cited by** 381 article(s) on the ISI Web of Science.

This article has been **cited by** 3 articles hosted by HighWire Press; see:
http://www.sciencemag.org/cgi/content/full/287/5455/1016#otherarticles

This article appears in the following **subject collections**:
Physics
http://www.sciencemag.org/cgi/collection/physics

Science (print ISSN 0036-8075; online ISSN 1095-9203) is published weekly, except the last week in December, by the American Association for the Advancement of Science, 1200 New York Avenue NW, Washington, DC 20005. Copyright 2000 by the American Association for the Advancement of Science; all rights reserved. The title *Science* is a registered trademark of AAAS.

linear polarization were carried out with the spherical grating monochromator on the wiggler beam line 10.1 at the Stanford Synchrotron Radiation Laboratory (SSRL). Spectromicroscopy studies were carried out with the PEEM2 facility on beam line 7.3.1.1 at the Advanced Light Source (ALS) (*10*).
17. P. Kuiper, B. G. Searle, P. Rudolf, L. H. Tjeng, C. T. Chen, *Phys. Rev. Lett.* **70**, 1549 (1993).
18. D. Alders *et al.*, *Phys. Rev. B* **57**, 11623 (1998).
19. J. Lüning *et al.*, in preparation.
20. B. T. Thole, G. van der Laan, G. A. Sawatzky, *Phys. Rev. Lett.* **55**, 2086 (1985).
21. $\langle M^2 \rangle = S(S+1) + \langle M \rangle \coth(1/2\theta)$ with $\theta = -S(S+1)/3\langle M \rangle\, T/T_c$ in mean field approximation.
22. M. Eibschütz, S. Shtrikman, D. Treves, *Phys. Rev.* **156**, 562 (1967).
23. E. N. Abarra, K. Takano, F. Hellman, A. E. Berkowitz, *Phys. Rev. Lett.* **77**, 3451 (1996).
24. I. Lyubutin, T. Dimitrieva, A. Stepin, *J. Exp. Theor. Phys.* **88**, 590 (1999).
25. G. A. Prinz, *Science* **282**, 1660 (1998).

26. Supported by the Division of Chemical Sciences (SSRL) and the Division of Materials Science (ALS) of the Office of Basic Energy Sciences of the U.S. Department of Energy. J.W.S. and F.N. acknowledge support by the Swiss National Science Foundation. J.P.L. thanks I. K. Schuller for stimulating his interest in the exchange bias problem.

1 October 1999; accepted 15 December 1999

Molecules in a Bose-Einstein Condensate

Roahn Wynar, R. S. Freeland, D. J. Han, C. Ryu, D. J. Heinzen*

State-selected rubidium-87 molecules were created at rest in a dilute Bose-Einstein condensate of rubidium-87 atoms with coherent free-bound stimulated Raman transitions. The transition rate exhibited a resonance line shape with an extremely narrow width as small as 1.5 kilohertz. The precise shape and position of the resonance are sensitive to the mean-field interactions between the molecules and the atomic condensate. As a result, we were able to measure the molecule-condensate interactions. This method allows molecular binding energies to be determined with unprecedented accuracy and is of interest as a mechanism for the generation of a molecular Bose-Einstein condensate.

Bose-Einstein condensation of dilute atomic gases, first observed in 1995 (*1, 2*), has become a dynamic and wide-ranging field of research (*3*). Dilute gas condensates are similar in certain respects to previously studied systems such as superfluid liquid helium, but they also exhibit many qualitatively new features. Among the most important is that the atoms can bind together to form molecules. Molecular recombination in three-body collisions leads to atomic losses in Bose condensates (*4*), because molecular binding energy is converted into kinetic energy. However, it is also possible to form molecules coherently in a condensate through stimulated recombination in two-body collisions. In this case, the atoms and recombined molecules may form a two-species Bose-Einstein condensate consisting of both an atomic and a molecular component, and a very interesting class of coherent atomic and molecular matter wave phenomena is predicted to occur (*5–8*).

We now report molecular formation in a dilute gas Bose condensate through coherent stimulated recombination of atoms. Specifically, we created state-selected $^{87}Rb_2$ molecules by stimulated Raman free-bound transitions in an ^{87}Rb atomic condensate (*9*). The molecules were created with a negligible kinetic energy and a potential energy of the order of the chemical potential (~100 nK) of the atomic Bose condensate. We probed the molecules spectroscopically through measurements of the stimulated Raman transition rate. This rate displayed a resonance line shape with a width as small as 1.5 kHz and more than 10,000 times narrower than those of similar resonances previously measured in a laser-cooled gas (*10, 11*). This narrow width is a direct consequence of the vanishing kinetic energy spread of the Bose condensate, and it allowed us to measure the molecular binding energy with unprecedented accuracy. We found that the molecule-condensate interactions shift and broaden the transition resonance and, as a result, we could measure these interactions.

Cold molecules have been produced and detected previously through photoassociation of laser-cooled atoms (*12*). In contrast to our work here, these molecules were formed incoherently in many different ro-vibrational levels and had a relatively large kinetic energy spread on the order of 100 μK. Our work is more closely related to previous experimental studies of Feshbach resonances, which demonstrated dramatic modifications to the interactions between ultracold atoms (*13*). In such a resonance, a molecular level very near the dissociation limit plays a role as a transient intermediate state in a collision of two atoms. In principle, Feshbach resonances can lead to the same class of phenomena as the stimulated Raman free-bound coupling we explore here. In either kind of experiment, if the molecular level has a sufficiently long lifetime, its effect on the gas cannot be understood simply through the resonant modification of the two-body interaction. Instead, the molecules must be treated as a separate population with its own properties and interactions with the atomic gas. We realize this regime in our experiment.

The stimulated Raman process is illustrated in Fig. 1. The condensate is illuminated with two laser fields 1 and 2 of frequency ω_1 and ω_2, wavevector $\vec{k}_1$ and $\vec{k}_2$, and intensity I_1 and I_2, respectively. A close pair of atoms from the condensate in a continuum state $|f\rangle$ interacts through a potential $V_g(R)$. This pair simultaneously absorbs a photon from laser field 1, emits a photon into laser field 2, and undergoes a transition to a molecular bound state $|g\rangle$ of binding energy ε. The process becomes resonant when $\Delta\omega = \omega_2 - \omega_1 = \varepsilon$. This resonance condition is satisfied for only a single molecular ro-vibrational state, so only that state is formed. The momentum transferred from the photons to the molecule in this process is $\hbar(\vec{k}_1 - \vec{k}_2)$, and is almost exactly zero in our experiment, because the laser beams propagate in the same direction and have a very small frequency difference. Because the atoms in the condensate are almost perfectly at rest, the molecules are formed almost perfectly at rest inside the atomic condensate.

Our measurements were carried out in a Bose-condensed gas of $^{87}Rb\ 5^2S_{1/2}(f = 1, m_f = -1)$ atoms confined in a magnetic trap. Here, f and m_f give the total spin and spin projection quantum numbers of the atoms. Our method to produce a condensate is similar to that first demonstrated by Anderson *et al.* (*1*), and has been described previously (*14*). The atoms were first captured in an optical trap in a high vacuum and were laser-cooled, then were transferred to a magnetic "TOP" trap (*1*) and further cooled with radio frequency–induced evaporation. The number of atoms, the gas temperature, and the fraction of the atoms in the condensate were measured with a laser-absorption imaging technique. For highly evaporated clouds, we could produce a gas with a temperature below 130 nK, condensate fraction greater than 80%, condensate atom number $N_c = 3.6 \times 10^5$, and peak condensate density $n_0 = 2.7 \times 10^{14}\ \mathrm{cm}^{-3}$ in a harmonic trapping potential $V_a(\vec{r}) = M\omega_r^2(x^2 + y^2)/2 + M\omega_z^2 z^2/2$, with $\omega_r/2\pi = 54$ Hz, $\omega_z/2\pi = 153$ Hz, and M the mass of an ^{87}Rb atom. We also produced condensates with a smaller atom number and density by continuing the evaporation further and by adiabatically lowering the trapping frequencies.

After the production cycle, we illuminated the condensate with the two laser fields for a period τ between 150 and 550 ms, with the trap left on. The TOP rotating magnetic field ampli-

---

Department of Physics, The University of Texas, Austin, TX 78712, USA.

*To whom correspondence should be addressed. E-mail: heinzen@physics.utexas.edu

tude was 4.8 G. The first laser beam, of frequency $\omega_1 \approx 2\pi c \times 12{,}555$ cm^{-1}, was tuned $\Delta_1/2\pi = 150$ MHz below resonance with the free-bound transition $|f\rangle \rightarrow |e\rangle$, where $|e\rangle = |0_g^-(\sim 5^2S_{1/2} + 5^2P_{1/2}); v, J = 0\rangle$ is an excited ro-vibrational level with a binding energy of 23 cm^{-1}. The important features of this transition have been discussed previously (*11, 15*). The level $|e\rangle$ is not directly populated to any significant degree. The second laser field was generated by acousto-optical modulation from the first, so that the jitter in $\Delta\omega$ was negligible. Both laser beams were linearly polarized along the TOP trap symmetry axis and were focused to waists of about 200 μm, much larger than the condensate size of about 10 μm. After the illumination period, we measured the number of atoms $N(\tau)$ in the trap with laser-induced fluorescence. This fluorescence signal was normalized to that obtained with no illumination period, and therefore provided the fraction of atoms $N(\tau)/N(0)$ remaining in the trap after the illumination period. In order to measure the spectrum of the stimulated Raman transition rate, we repeated this measurement for a succession of values of $\Delta\omega$.

Typical spectra are shown in Fig. 2. For most values of $\Delta\omega$, the laser illumination has no effect on the condensate. However, we did observe a strong loss of atoms from the trap near $\Delta\omega/2\pi = 636$ MHz. This loss occurs because the lasers resonantly drive stimulated Raman transitions to the molecular bound state $|g\rangle$, and these molecules are subsequently lost from the trap at a rate γ_2. This state is the second-to-last vibrational level belonging to the $F = 2$, $M_F = -2$, $l = 0$ potential which connects with the $5^2S_{1/2}(f = 1, m_f = -1) + 5^2S_{1/2}(f = 1, m_f = -1)$ dissociation limit, where F and M_F are the total spin and spin projection quantum numbers of the molecule, respectively, and l is the rotational quantum number. The analysis of similar bound states has been discussed for the case of $^{85}Rb_2$ (*11, 15*).

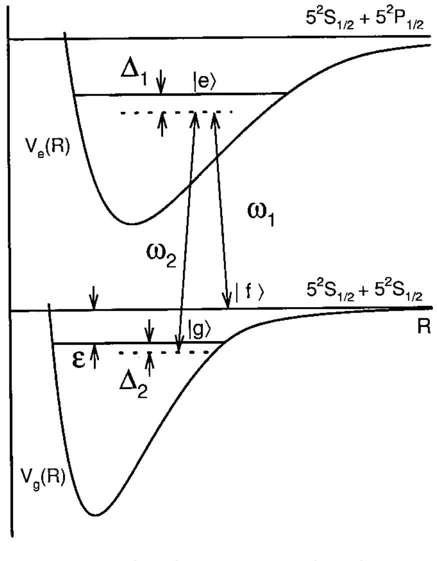

Fig. 1. Stimulated Raman coupling between free and bound states of atoms in a Bose-Einstein condensate.

The transition linewidth is remarkably narrow, because the usual spectroscopic broadening mechanisms are absent. The width of the Raman transition depends only on the widths of the initial and final states $|f\rangle$ and $|g\rangle$ which are radiatively stable because Rb_2 is homonuclear. Both Doppler broadening and the kinetic energy spread of the colliding atoms are negligible due to the extremely low kinetic energies ($\ll \hbar\omega_z/k_B = 7$ nK) of the atoms in the Bose condensate. The kinetic energy of the thermally excited atoms plays a negligible role, because their number and collision rate are small relative to the Bose-condensed atoms. We have measured the Zeeman shift of the transition frequency to be <1.5 kHz/G, so there is no broadening due to spatial or time variations of the magnetic field. The Zeeman shift is negligible because the molecular magnetic moment is equal to the combined magnetic moment of the two atoms.

The dominant perturbations to the molecular level $|g\rangle$ at high laser intensities are an AC Stark shift $\Delta\varepsilon_L \approx \beta[I_1/(\Delta_1 + \varepsilon) + I_2/\Delta_1]$ and a broadening $\gamma_L \approx \beta\gamma_1[I_1/(\Delta_1 + \varepsilon)^2 + I_2/\Delta_1^2]$ induced by the laser couplings to the $|g\rangle \leftrightarrow |e\rangle$ transition, where $\gamma_1 = 2\pi \times 12$ MHz is the spontaneous emission rate of level $|e\rangle$ and β is a constant. The results of our measurements of this shift and broadening for different intensities are shown in Fig. 3. The plotted values result from a fit of the measured trap-loss line shapes to a simple model of the atomic loss in which the stimulated Raman transition is assumed to be centered at frequency ε' and homogeneously broadened with a width γ_2'. The broadening is not power broadening in the usual sense; it arises from spontaneous Raman scattering of the laser photons by the molecules, which removes them from the condensate and limits their lifetime. The solid lines show the values calculated from the expressions given above, by taking best-fit values of β and the two zero-intensity intercepts. The nonzero intercept for γ_2' indicates that an additional broadening mechanism is present.

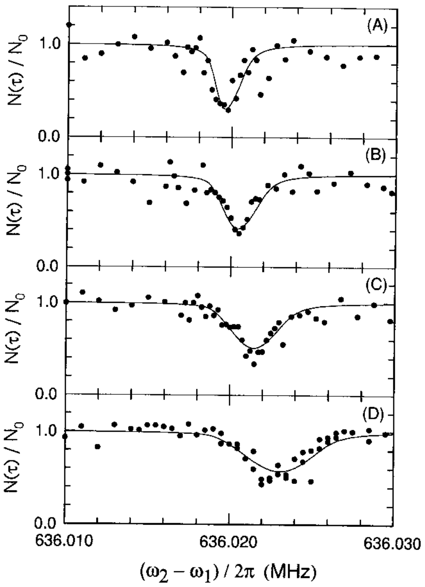

Fig. 2. Stimulated Raman free-bound transition line shapes in a Bose-Einstein condensate for four different peak condensate densities: (**A**) $n_0 = 0.77 \times 10^{14}$ cm^{-3}; (**B**) $n_0 = 1.22 \times 10^{14}$ cm^{-3}; (**C**) $n_0 = 1.75 \times 10^{14}$ cm^{-3}; and (**D**) $n_0 = 2.60 \times 10^{14}$ cm^{-3}. Each spectrum shows the fraction of atoms remaining in the condensate after illumination by the two coherent laser fields, as a function of the laser frequency difference. The resonant decrease in atom number arises from the formation of molecules by stimulated Raman free-bound transitions, followed by their subsequent loss from the trap. The increase in width and center frequency of the resonance with density arise from the atom-condensate and molecule-condensate mean-field interactions.

At the lowest laser intensities, the transition becomes sensitive to molecule-condensate interactions. We determined this with measured line shapes for four different trap frequencies and three different stopping conditions for the evaporation, which yielded condensate numbers N_c ranging from 140,000 to 360,000 and peak condensate densities n_0 at $\tau = 0$ ranging from 0.77×10^{14} cm^{-3} to 2.7×10^{14} cm^{-3}. For these measurements, the laser intensities were held fixed at very low values $I_1 = 5.6$ W/cm^2 and $I_2 = 0.51$ W/cm^2, which yields $\Delta\varepsilon_L/2\pi = 9.5$ kHz, and $\gamma_L/2\pi = 350$ Hz. In all cases, the condensate fraction was initially >80%, and

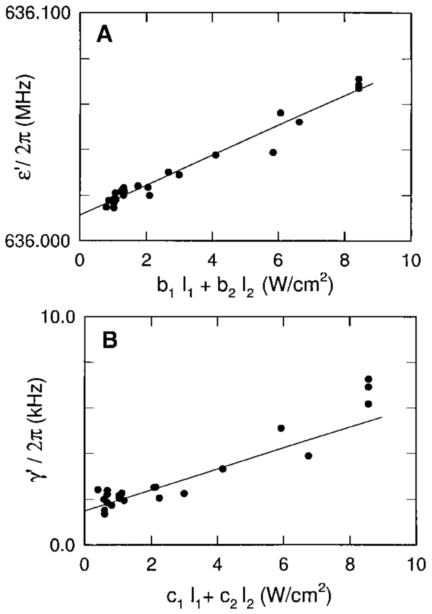

Fig. 3. (**A**) Center frequency ε' and (**B**) width γ' of the stimulated Raman free-bound resonance as a function of the weighted average laser intensity. The coefficients $b_1 = 0.160$, $b_2 = 0.840$, $c_1 = 0.035$, and $c_2 = 0.965$ are proportional to the laser detuning factors discussed in the text.

>70% throughout the laser illumination period, as established by independent measurements. Figure 2 shows a sample of four of these line shapes that span the full range of densities.

The transition line shapes show a clear dependence on condensate density. This density dependence arises from elastic and inelastic interactions of both the initial pair of atoms and the molecule with the condensate atoms. Both the elastic and inelastic scattering properties can be described in terms of complex two-body scattering lengths (*16*) $a_{ia} = a'_{ia} - ia''_{ia}$, where $i = a$ for the atom-atom scattering and $i = m$ for the molecule-atom scattering. The inelastic interactions between the Bose-condensed ^{87}Rb atoms are negligible, so that $a''_{aa} \ll |a'_{aa}|$, but inelastic atom-molecule collisions $\mathrm{Rb}_2(v,l,F,M_F) + \mathrm{Rb}(f,m_f) \rightarrow \mathrm{Rb}_2(v',l',F',M'_F) + Rb(f',m'_f)$ could occur at a significant rate $\mathrm{K}_{inel}\mathrm{n}(\vec{r})$, where $\mathrm{n}(\vec{r})$ is the atomic density, $\mathrm{K}_{inel} = 4\pi\hbar a''_{ma}/\mu_{ma}$ is the collision rate constant, and $\mu_{ma} = 2\mathrm{M}/3$ is the reduced mass for a molecule-atom pair. These collisions could be inelastic in any of the internal degrees of freedom including molecular rotation or vibration, and they would eject the molecule and atom from the condensate due to the conversion of internal energy to kinetic energy. They would also give rise to a finite lifetime of the molecules and to a broadening of the Raman transition line shape.

The elastic interactions of the particles with the atomic condensate are more subtle (Fig. 4). They give rise to a mean-field contribution $\mathrm{U}_{ia}(\vec{r}) = g_i\mathrm{n}(\vec{r})$ to the chemical potential of an atom ($i = a$) or molecule ($i = m$) in the condensate, where $g_i = 2\pi\hbar^2 a'_{ia}/\mu_{ia}$, and $\mu_{aa} = M/2$ is the reduced mass of an atom pair. This expression follows from the substitution of the complex scattering length into coupled field equations describing the mixed atomic and molecular gas (*5–8, 17*). The value of $a'_{aa} = 104\ a_0$ is known from previous measurements (*18*), where a_0 is the atomic unit of length, whereas the values of a'_{ma} and a''_{ma} are unknown. We assume that the condensate is well described by the Thomas-Fermi approximation (*19*). In this limit, the kinetic energy of the atoms is negligible, and both $\mathrm{n}(\vec{r})$ and U_{aa} are proportional to a constant minus the parabolic trap potential. In addition, the sum $2\mathrm{U}_{Ta} = 2\mathrm{U}_{aa} + 2\mathrm{V}_a$ of the mean-field and trap potential energy of a pair of atoms is independent of position (*19*). The trap potential for a molecule in our case is $\mathrm{V}_m = 2\mathrm{V}_a$. The mean-field energy U_{ma} of a molecule also follows the inverted parabolic form of $\mathrm{n}(\vec{r})$, but with an unknown coefficient. Therefore, the sum $\mathrm{U}_{Tm} = \mathrm{U}_{ma} + \mathrm{V}_m$ of the mean-field and trap potential energy of a molecule is spatially inhomogeneous. The change in energy in converting two atoms into one molecule, not including internal energy, is $\Delta\mathrm{U} = 2\mathrm{U}_{Ta} - \mathrm{U}_{Tm} = \Delta g\mathrm{n}$, where $\Delta g = 2g_a - g_m$. This energy difference depends on position in the trap, and it gives rise to a density-dependent shift of the stimulated Raman transition and to an inhomogeneous broadening of its width (Fig. 4). Similar shifts and broadenings have been observed in a two-photon transition between atomic states in a hydrogen Bose-Einstein condensate (*20*).

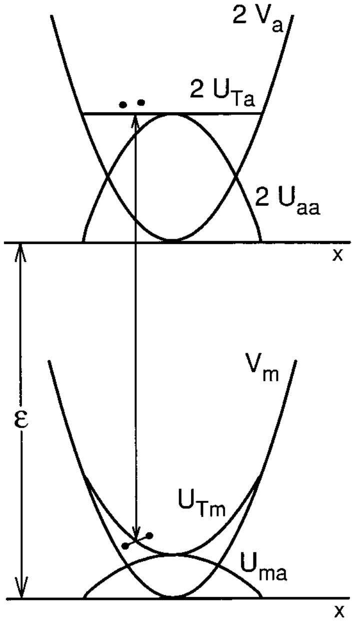

Fig. 4. Mean-field and trap energies for atoms and molecules in the atomic condensate, illustrating the inhomogeneous mean-field shifts of the stimulated Raman resonance.

To analyze these line shapes, we divided the data into three sets of line shapes corresponding to the three different evaporation stopping conditions. We carried out a simultaneous nonlinear least squares fit of all line shapes in each data set to a model of the trap loss. We assumed that the loss of atomic density is given by $d\mathrm{n}(\vec{r},t)/dt = -\mathrm{K}_{PA}\bar{N}\mathrm{n}(\vec{r},t)^2$. In this expression, $\mathrm{K}_{PA} = \mathrm{K}_0(\gamma_L\gamma_2(\vec{r},t)/4)/[(\Delta\omega - \varepsilon(\vec{r},t))^2 + (\gamma_2(\vec{r},t)/2)^2]$ is the rate constant for stimulated Raman photoassociation, with $\varepsilon(\vec{r},t) = \varepsilon_0 + \Delta\varepsilon_L + \Delta g\mathrm{n}(\vec{r},t)/\hbar$, and $\gamma_2(\vec{r},t) = \gamma_L + \mathrm{K}_{inel}\mathrm{n}(\vec{r},t)$. This form for K_{PA} follows from the zero-temperature and large Δ_1 limit of two-color photoassociation theory (*21*), or from a damped limit of coupled atomic-molecular condensate theory (*5–8, 17*). In this expression, ε_0 is the unperturbed value of the molecular binding energy and $\bar{N}(\vec{r},t) = (2\gamma_L + 3\mathrm{K}_{inel}\mathrm{n})/\gamma_2$ is the average number of atoms lost per stimulated Raman photoassociation event, accounting for the subsequent loss of an additional atom in an inelastic atom-molecule collision. We also assumed that the initial condensate fraction was 0.9, that the atoms were lost only from the condensate, and that the condensate maintained a Thomas-Fermi density distribution throughout the illumination period. The fit parameters are the values of K_0, ε_0, a'_{ma}, and K_{inel} for each data set. The curves in Fig. 2 show the calculated line shapes for the best-fit parameters from the corresponding data set and are in very good agreement with the data. From this analysis, we obtained $\varepsilon_0/2\pi = 636.0094 \pm 0.0012$ MHz, $a'_{ma} = -180 \pm 150\ a_0$, $\mathrm{K}_{inel} < 8 \times 10^{-11}$ cm^3/s, $a''_{ma} < 110\ a_0$, and $\mathrm{K}_0 = 9 \times 10^{-14}$ cm^3/s. The error bars include contributions from statistical error corresponding to approximately two standard deviations, and from estimated uncertainties in atom number, light shift, and possible effects of thermally excited atoms, added in quadrature. The results from the three data sets are consistent to within the stated error limits.

Our results show that the mean-field shifts are responsible for the shift and for most of the broadening of the line shapes, and that this broadening is inhomogeneous. The negative value of a'_{am} implies that the mean-field interactions tend to increase the strength of the trapping potential for the molecules. We do not obtain firm evidence for a nonzero inelastic collision rate. Within our allowed range for K_{inel}, the lifetime γ_2^{-1} of the molecules at a density $\mathrm{n} = 1 \times 10^{14}$ cm^{-3} could lie anywhere in the range from 0.10 to 0.45 ms. Thus, their lifetime is much less than one vibration period in the potential $\mathrm{U}_{Tm}(\vec{r})$, which justifies our assumptions that the stimulated Raman transitions occur at a well-defined position, and that any subsequent atom-molecule collision also occurs at that same position. For molecular lifetimes much longer than the trap vibration period, the spectrum would instead consist of discrete transitions between the ground vibrational state of the initial pair of atoms in the potential $2\mathrm{U}_{Ta}$ and the quantized vibrational levels of the trapped molecule in the potential U_{Tm}. Because these transitions can be spaced by several hundred hertz, it may be possible to produce a molecular gas in its ground state, i.e., a molecular condensate, by resolving the transition to the lowest trap vibrational state. The molecular density when the interaction is resonant is $\mathrm{n}_m = \mathrm{K}_0\mathrm{n}^2\gamma_L/\gamma_2^2$ and for our conditions is at most 1.1% of the atomic density, which justifies our neglect of the molecule-molecule interactions.

The atom-molecule interactions are of great interest in their own right. They are expected to exhibit a wide range of interesting resonance and threshold phenomena (*16, 22, 23*). The collisional interactions should depend very strongly on the molecular rovibrational state; in particular, the inelastic rates are likely to decrease rapidly with increasing molecular binding energy (*22*). Rotating molecules could exhibit anisotropic interactions. Further, measurements of these interactions, including those presented here, are of great interest for theoretical studies of possible mixed atomic and molecular Bose condensates.

Interesting directions for future work include investigations of output coupling of the molecules from the condensate, the formation of other bound states, and the dependence of the molecule-condensate interactions on the ro-vibrational state of the molecule. The binding energies of the highest 5 to 10 vibrational bound states could be measured to a precision of about 10^{-7} cm^{-1}, which would provide extremely precise information on the long-range atomic interactions. The molecular cloud might be directly imaged. It should be possible to realize the limit in which the stimulated transition rate exceeds the molecular decay rate (*8*). In this regime, reversible formation of a molecular Bose condensate from an atomic condensate could occur (*5*–*8*), and further studies of mixed atom-molecular condensates and nonlinear matter wave phenomena would be feasible.

References and Notes

1. M. H. Anderson *et al.*, *Science* **269**, 198 (1995).
2. C. C. Bradley *et al.*, *Phys. Rev. Lett.* **75**, 1687 (1995); K. B. Davis *et al.*, *Phys. Rev. Lett.* **75**, 3969 (1995).
3. M. Inguscio, S. Stringari, C. E. Wieman, Eds., *Bose-Einstein Condensation in Atomic Gases*, Proceedings of the 1998 Enrico Fermi Summer School, Course CXL (IOS Press, Amsterdam, 1999).
4. E. A. Burt *et al.*, *Phys. Rev. Lett.* **79**, 337 (1997); D. M. Stamper-Kurn *et al.*, *Phys. Rev. Lett.* **80**, 2027 (1998).
5. P. D. Drummond, K. V. Kheruntsyan, H. He, *Phys. Rev. Lett.* **81**, 3055 (1998).
6. J. Javanainen and M. Mackie, *Phys. Rev. A* **59**, R3186 (1999).
7. E. Timmermans *et al.*, *Phys. Rev. Lett.* **83**, 2691 (1999).
8. D. J. Heinzen, R. H. Wynar, P. D. Kheruntsyan, P. D. Drummond, unpublished results.
9. P. S. Julienne *et al.*, *Phys. Rev. A* **58**, R797 (1998).
10. E. R. I. Abraham *et al.*, *Phys. Rev. Lett.* **74**, 1315 (1995).
11. C. C. Tsai *et al.*, *Phys. Rev. Lett.* **79**, 1245 (1997).
12. A. Fioretti *et al.*, *Phys. Rev. Lett.* **80**, 4402 (1998); A. N. Nikolov *et al.*, *Phys. Rev. Lett.* **82**, 703 (1999); T. Takekoshi *et al.*, *Phys. Rev. A* **59**, R5 (1999).
13. S. Inouye *et al.*, *Nature* **392**, 151 (1998); Ph. Courteille *et al.*, *Phys. Rev. Lett.* **81**, 69 (1998); J. L. Roberts *et al.*, *Phys. Rev. Lett.* **81**, 5109 (1998); V. Vuletić *et al.*, *Phys. Rev. Lett.* **82**, 1406 (1999).
14. D. J. Han *et al.*, *Phys. Rev. A* **57**, R4114 (1998).
15. J. R. Gardner *et al.*, *Phys. Rev. Lett.* **74**, 3764 (1995); H. M. J. M. Boesten *et al.*, *J. Phys. B* **32**, 287 (1999).
16. N. Balakrishnan *et al.*, *Chem. Phys. Lett.* **280**, 5 (1997).
17. F. A. Van Abeelen and B. J. Verhaar, *Phys. Rev. Lett.* **83**, 1550 (1999); V. A. Yurovsky *et al.*, *Phys. Rev. A* **60**, R765 (1999).
18. J. M. Vogels *et al.*, *Phys. Rev. A* **56**, R1067 (1997); P. S. Julienne *et al.*, *Phys. Rev. Lett.* **78**, 1880 (1997).
19. F. Dalfovo *et al.*, *Rev. Mod. Phys.* **71**, 463 (1999).
20. D. G. Fried *et al.*, *Phys. Rev. Lett.* **81**, 3811 (1998).
21. J. L. Bohn and P. S. Julienne, *Phys. Rev. A* **60**, 414 (1999).
22. N. Balakrishnan *et al.*, *Phys. Rev. Lett.* **80**, 3224 (1998).
23. R. C. Forrey *et al.*, *Phys. Rev. A* **58**, R2645 (1998); R. C. Forrey *et al.*, *Phys. Rev. Lett.* **82**, 2657 (1999).

24. We gratefully acknowledge support by NSF, the R. A. Welch Foundation, and the NASA Microgravity Research Division.

12 November 1999; accepted 13 December 1999

Zener Model Description of Ferromagnetism in Zinc-Blende Magnetic Semiconductors

T. Dietl,[1,2]* H. Ohno,[1]* F. Matsukura,[1] J. Cibert,[3] D. Ferrand[3]

Ferromagnetism in manganese compound semiconductors not only opens prospects for tailoring magnetic and spin-related phenomena in semiconductors with a precision specific to III-V compounds but also addresses a question about the origin of the magnetic interactions that lead to a Curie temperature (T_C) as high as 110 K for a manganese concentration of just 5%. Zener's model of ferromagnetism, originally proposed for transition metals in 1950, can explain T_C of $Ga_{1-x}Mn_xAs$ and that of its II-VI counterpart $Zn_{1-x}Mn_xTe$ and is used to predict materials with T_C exceeding room temperature, an important step toward semiconductor electronics that use both charge and spin.

Advances in the epitaxy of III-V semiconductor compounds now make it possible to fabricate quantum structures in which confined electrons or photons exhibit outstanding properties and functionalities. The atomic precision of deposition and processing has made it possible to observe and examine quantum Hall effects, dot and microcavity semiconductor lasers, and single-electron charging phenomena, to name only a few from many other recent developments (*1*). Therefore, the discovery of ferromagnetism in (In,Mn)As (*2*) and then in (Ga,Mn)As (*3*) enables examination of collective magnetic phenomena in a well-controlled environment. At the same time, applications in sensors and memories as well as for computing with electron spins can be envisaged (*4*). It is then important to understand the ferromagnetism in these semiconductors and to ask whether the T_C's can be raised to above 300 K from the present 110 K (*3*).

Our theory considers ferromagnetic correlation mediated by holes originating from shallow acceptors in the ensemble of the localized spins in doped magnetic semiconductors. The magnetic ion Mn, which occupies the cation (Ga) sublattice in zinc-blende $Ga_{1-x}Mn_xAs$ (*5*), provides a localized spin and at the same time acts as an acceptor. These Mn acceptors compensate the deep antisite donors commonly present in GaAs grown by low-temperature molecular beam epitaxy and produce a p-type conduction with metallic resistance for the Mn concentration x in the range $0.04 \leq x \leq 0.06$ (*6*, *7*). According to optical studies, Mn in GaAs forms an acceptor center characterized by a moderate binding energy (*8*), $E_a = 110$ meV, and a small magnitude of the energy difference between the triplet and singlet state of the bound hole (*8*, *9*), $\Delta\varepsilon = 8 \pm 3$ meV. This value demonstrates that the hole introduced by the divalent Mn does not occupy d shell or form a Zhang-Rice–like singlet (*10*) so that, despite a strong p-d hybridization, (Ga,Mn)As can be classified as a charge-transfer insulator, a conclusion confirmed by photoemission spectroscopy (*11*).

Zener (*12*) first proposed the model of ferromagnetism driven by the exchange interaction between carriers and localized spins. However, this model was later abandoned, as neither the itinerant character of the magnetic electrons nor the quantum (Friedel) oscillations of the electron spin polarization around the localized spins were taken into account; both of these are now established to be critical ingredients for the theory of magnetic metals. We emphasize that in the case of semiconductors, however, the effect of the Friedel oscillations averages to zero because the mean distance between the carriers is greater than that between the spins. In such a case, the Zener model becomes equivalent (*13*) to the approach developed by Ruderman, Kittel, Kasuya, and Yosida (RKKY), in which the presence of the oscillations is taken explicitly into account.

We began by determining how the Ginzburg-Landau free-energy functional F depends on the magnetization M of the localized spins. In the case of the holes residing in the Γ_8 valence bands, spin-orbit coupling and the kp interaction, that is, the mixing of the angular momentum basis states associated with the delocalization of atomic orbitals, are expected to play an important role. Therefore, we computed the carrier contribution to F, $F_c[M]$, by diagonalizing the 6×6 Kohn-Luttinger matrix (*14*) together with the p-d exchange contribution (*15*) and by integrating over the rather anisotropic Fermi volume (inset, Fig. 1). The model allows for the presence of strain and arbitrary orientations of M. Standard values of the Luttinger parameters γ_i and the spin-orbit splitting Δ_o were taken as input parameters (*16*). Ac-

---

[1] Research Institute of Electrical Communication, Tohoku University, Katahira 2-1-1, Sendai 980-8577, Japan. [2] Institute of Physics and College of Science, Polish Academy of Sciences, al. Lotników 32/46, PL-02668 Warsaw, Poland. [3] Laboratoire de Spectrométrie Physique, Université Joseph Fourier Grenoble 1-CNRS (UMR 5588), F-38402 Saint Martin d'Hères Cedex, France.

*To whom correspondence should be addressed. E-mail: dietl@ifpan.edu.pl; ohno@riec.tohoku.ac.jp